KIR3DL1 Allotype-Dependent Modulation of NK Cell Immunity against Chronic Myeloid Leukemia

Kiyotaka Izumi, Takero Shindo, Huong Thi Ngo, Kaori Nakayama-Hosoya, Koshi Akahane, Minori Tamai, Thao T. T. Nguyen, Ai Kawana-Tachikawa, Takeshi Inukai and Akifumi Takaori-Kondo

ImmunoHorizons 2021, 5 (8) 687-702
doi: https://doi.org/10.4049/immunohorizons.2100054
http://www.immunohorizons.org/content/5/8/687

ImmunoHorizons is an open access journal published by
The American Association of Immunologists, Inc.,
1451 Rockville Pike, Suite 650, Rockville, MD 20852

ISSN 2573-7732.

ImmunoHorizons

RESEARCH ARTICLE

Clinical and Translational Immunology

KIR3DL1 Allotype-Dependent Modulation of NK Cell Immunity against Chronic Myeloid Leukemia

Kiyotaka Izumi,* Takero Shindo,* Huong Thi Ngo,* Kaori Nakayama-Hosoya,† Koshi Akahane,‡ Minori Tamai,‡ Thao T. T. Nguyen,‡ Ai Kawana-Tachikawa,† Takeshi Inukai,‡ and Akifumi Takaori-Kondo*

*Department of Hematology and Oncology, Kyoto University Graduate School of Medicine, Kyoto, Japan; †AIDS Research Center, National Institute of Infectious Diseases, Tokyo, Japan; and ‡Department of Pediatrics, School of Medicine, University of Yamanashi, Chuo, Japan

ABSTRACT

Tyrosine kinase inhibitor (TKI)–treated chronic myeloid leukemia (CML) patients with increased NK cell number have a better prognosis, and thus, NK cells may suppress CML. However, the efficacy of TKIs varies for reasons yet to be fully elucidated. As NK cell activity is modulated by interactions between their killer cell Ig-like receptors (KIRs) and HLAs of target cells, the combination of their polymorphisms may have functional significance. We previously showed that allelic polymorphisms of *KIR3DL1* and *HLAs* were associated with the prognosis of TKI-treated CML patients. In this study, we focus on differential NK cell activity modulation through KIR3DL1 allotypes. KIR3DL1 expression levels varied according to their alleles. The combination of KIR3DL1 expression level and HLA-Bw4 motifs defined NK cell activity in response to the CML-derived K562 cell line, and Ab-mediated KIR3DL1 blocking reversed this activity. The TKI dasatinib enhanced NK cell activation and cytotoxicity in a KIR3DL1 allotype-dependent manner but did not significantly decrease effector regulatory T cells, suggesting that it directly activated NK cells. Dasatinib also enhanced NK cell cytotoxicity against K562 bearing the BCR-ABL1 T315I TKI resistance–conferring mutation, depending on KIR3DL1/HLA-Bw4 allotypes. Transduction of *KIR3DL1*01502* into the NK cell line NK-92 resulted in KIR3DL1 expression and suppression of NK-92 activity by HLA-B ligation, which was reversed by anti-KIR3DL1 Ab. Finally, KIR3DL1 expression levels also defined activation patterns in CML patient–derived NK cells. Our findings raise the possibility of a novel strategy to enhance antitumor NK cell immunity against CML in a KIR3DL1 allotype-dependent manner. *ImmunoHorizons*, 2021, 5: 687–702.

INTRODUCTION

Although tyrosine kinase inhibitors (TKIs) have greatly improved the outcome of patients with chronic myeloid leukemia (CML) (1,2), several problems remain to be solved. Some cases acquire TKI resistance through mutation, such as T315I in the ABL kinase domain (3). Long-term TKI treatment impairs the quality of life for the majority of CML patients (4), and the cost of life-long TKI treatment is considerable (5,6). Interestingly, a minority of cases experience long-term deep molecular remission without TKI maintenance, a status designated as treatment-free remission (7). However, the probability of treatment-free remission is

Received for publication August 4, 2021. Accepted for publication August 4, 2021.

Address correspondence and reprint requests to: Dr. Takero Shindo, Department of Hematology and Oncology, Kyoto University Graduate School of Medicine, 54 Kawahara-cho, Shogo-in, Sakyo-ku, Kyoto 606-8507, Japan. E-mail address: takeros@kuhp.kyoto-u.ac.jp

ORCIDs: 0000-0002-2085-6151 (T.S.); 0000-0001-5093-167X (T.T.T.N.); 0000-0002-3082-5324 (A.K.-T.); 0000-0001-7678-4284 (A.T.-K.).

This work was supported by research grants of Japan Society for the Promotion of Science KAKENHI Grant 19K08812 (to T.S.), the Translational Research Program-Strategic Promotion for Practical Application of Innovative Medical Technology from the Japan Agency for Medical Research and Development (to T.S.), grants-in-aid from the Uehara Memorial Foundation (to T.S.), Novartis Pharmaceuticals Foundation (to T.S. and A.T-K.), and Bristol-Myers Squibb Foundation (to T.S. and A.T.-K.). A. T-K. received research funds and lecture fees from Takeda Pharmaceutical, Otsuka Pharmaceutical, and Pfizer.

The online version of this article contains supplemental materials.

Abbreviations used in this article: AML, acute myeloid leukemia; cat., catalog; CML, chronic myeloid leukemia; CTV, CellTrace Violet; ID, identifier; K562-null, HLA-null K562; KIR, killer cell Ig-like receptor; KIR3DL1-high donor, donor with other alleles including **01502* showed high MFI of Z27; KIR3DL1-low donor, donor with *KIR3DL1*00701* showed low MFI of Z27; MFI, mean fluorescence intensity; TKI, tyrosine kinase inhibitor; Treg, regulatory T cell.

The online version of this article contains supplemental materials.

https://doi.org/10.4049/immunohorizons.2100054

limited, and its predictive determinants are unclear. Given that several reports show positive correlations between increased NK cell number and successful discontinuation of TKIs (8,9), antitumor NK cell immunity may underlie the CML suppression. Understanding their mode of action against CML would enable safer discontinuation of TKIs and help to overcome TKI resistance. Furthermore, elucidating determinants of antitumor NK cell immunity would help to establish a novel immunotherapy, which may also be applicable to many other malignancies.

NK cell activity is modulated through interactions between several kinds of NK cell receptors and their ligands on target cells. In particular, the killer cell Ig-like receptors (KIRs) constitute a major subset, and these stimulate or inhibit NK cell activity by ligation with specific HLA class I molecules. Ligation of inhibitory NK cell receptors with their HLA class I ligands is indispensable for educating NK cells (10), after which NK cells can attack HLA-deficient cells by recognition of "missing self" (11). Inhibitory KIRs are involved in the education process along with CD94/NKG2A, which recognizes HLA-E (12). *KIR* genes are encoded on human chromosome 19. Each of them shows abundant allelic polymorphism (13,14), but their functional significance is largely unknown.

KIR3DL1 is one of the inhibitory KIRs, and its known ligands are HLA-A and HLA-B molecules that contain Bw4 motifs (15). HLA-B molecules are classified into Bw4 or Bw6 subtypes based on the sequence of amino acids between positions 77 and 83 in the α1 helix (16,17). According to the amino acid at position 80, Bw4 motifs are further divided into Bw4-80I (isoleucine) and Bw4-80T (threonine) motifs (18). KIR3DL1 has abundant allelic polymorphism. Its alleles are classified into high, low, and null allotypes, depending on surface expression levels (19–22). In vitro experiments have revealed some residues that vary among KIR3DL1 allotypes define their affinity for ligands and surface expression levels (23). KIR3DL1 and HLA-B allotypes differentially modulate NK cell activation (24–28). Their stronger interaction avidity was associated with greater NK cell suppression (25).

Several studies have raised the possible clinical significance of interaction avidity between KIR3DL1 and HLA-B proteins (29–31). According to these reports, interactions between KIR3DL1-low and Bw4-80T and KIR3DL1-high and Bw4-80I are defined as "strong" interactions between KIR3DL1-low and Bw4-80I, KIR3DL1-high and Bw4-80T are defined as "weak," and any pairs that contain KIR3DL1-null or Bw6 are defined as "non." Whereas the strong interaction showed a protective effect on disease progression in HIV-infected individuals (29), the weak or noninteractions correlated with a superior treatment response in neuroblastoma patients (30) and allogeneic transplant–treated acute myeloid leukemia (AML) patients (31). However, a recent study on AML failed to confirm this (32). Although the predicted levels of HLA class I expression on pathologic cells in different diseases may explain the difference (33), these conflicting results indicate that the clinical significance of the interaction strength still requires further verification.

We previously reported that the efficacy of TKIs in CML patients was associated with allelic polymorphisms of *KIRs* and *HLAs* in a Japanese cohort (34). In accordance with the previous studies of neuroblastoma and AML (30,31), noninteracting combinations of KIR3DL1 and HLA-B predicted earlier achievement of a deep molecular response. TKIs such as imatinib and dasatinib may enhance NK cell immunity by suppressing regulatory T cells (Tregs) (35,36). However, there are no data on how these drugs regulate NK cell immunity through KIR–HLA interactions. In this study, we performed functional analysis of KIR3DL1 allotypes on NK cells in vitro. In particular, we examined how dasatinib affects NK cell activity based on KIR–HLA interaction. Furthermore, we explored the potential of KIR3DL1 blockade to enhance antitumor NK cell immunity.

MATERIALS AND METHODS

Cell lines

K562 (RCB 1897), a CML-derived cell line that lacks expression of HLA class I, was purchased from RIKEN BRC Cell Bank (Tsukuba, Japan), and human NK cell line NK-92 (CRL-2407) was purchased from American Type Culture Collection (Manassas, VA). K562 cells were cultured in RPMI-1640 medium (Nacalai Tesque, Kyoto, Japan; catalog [cat.] no. 30264-85) supplemented with 10% FBS (Life Technologies, Thermo Fisher Scientific, Waltham, MA; cat. no. 10270), and 1% penicillin–streptomycin–glutamine (Nacalai Tesque; cat. no. 06168-34). NK-92 cells were cultured in α-MEM medium (Nacalai Tesque; cat. no. 21445-95) supplemented with 12.5% FBS, 12.5% horse serum (Life Technologies; cat. no. 16050122), 0.2 mM myo-inositol (Nacalai Tesque; cat. no. 13051-82), 0.1 mM 2-ME (FUJIFILM Wako Pure Chemical, Osaka, Japan; cat. no. 198-15781), 0.02 mM folic acid (Nacalai Tesque; cat. no. 16221-62), 1% penicillin–streptomycin (FUJIFILM Wako Pure Chemical; cat. no. 168-23191) and 100 U/ml recombinant human IL-2 (Shionogi, Osaka, Japan; cat. no. 6399411D1022).

Generation of the T315I knock-in K562 cell line

Introduction of the T315I mutation into K562 cells was performed by homologous recombination using the CRISPR/Cas9 system as previously described (37). In brief, single guide RNA (5′-aactcagtgatgatatagaacgg-3′), single-strand oligodeoxynucleotides (5′-cgttcacctcctgccggttgcactccctcaggtagtccaggaggttcccgtaggtcatgaaTtcGAtAatgatatagaacgggggctcccgggtgcagaccc-3′; capital letters indicate mutated nucleotides), and recombinant Cas9 protein (Integrated DNA Technologies, Coralville, IA; cat. no. 1074181) were electroporated into parental cells in the presence of 10 nM DNA ligase IV inhibitor SCR7 (Xcess Biosciences, San Diego, CA; cat. no. M60082-2S). To block recutting of repaired target loci, three additional silent point mutations were simultaneously introduced. Seven days after electroporation, the cells were cultured in the presence of 0.5 μM of imatinib (Selleck Chemicals, Houston; TX, cat. no. S1026). After

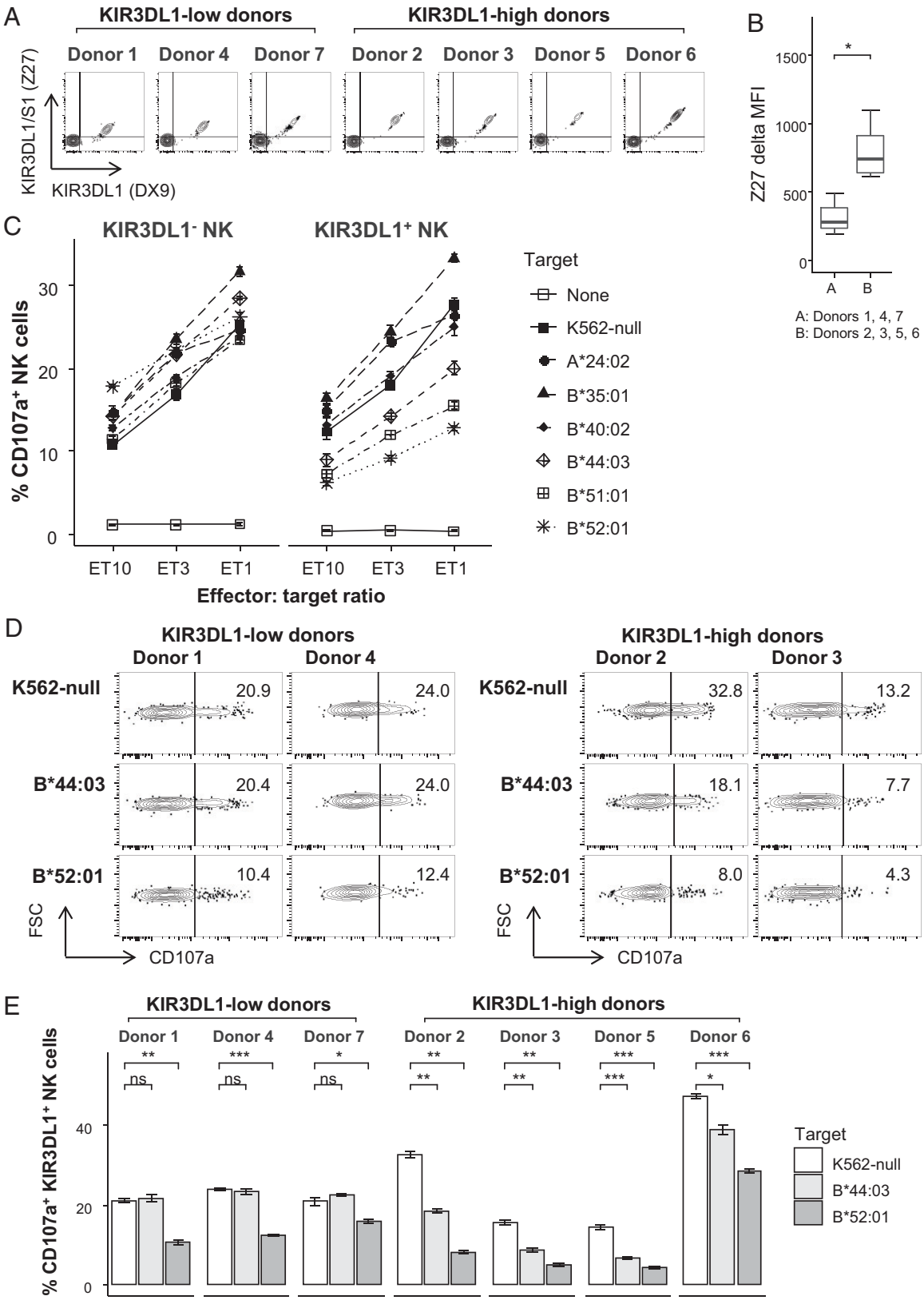

FIGURE 1. Activation of KIR3DL1+ NK cells depends on KIR3DL1 expression.

(**A**) Representative flow cytometry contour plots of KIR3DL1^{+} NK cells stained with Z27 and DX9 Abs. (**B**) The MFI of Z27 staining was compared. The difference in MFI (delta MFI) between positive and negative populations was calculated for each donor. Boxes represent interquartile range, horizontal lines in the boxes represent the median value, and whiskers indicate the minimum and the maximum values (*$p < 0.05$). (**C**) ***(Continued)***

https://doi.org/10.4049/immunohorizons.2100054

TABLE I. HLA-A and B and KIR3DL1 alleles of healthy donors in this study

Donor	HLA-A		HLA-B		KIR3DL1		Z27-MFI	KIR3DS1[a]
1	*A*02:01*	***A*24:02***	*B*35:01*	*B*54:01*	*00701	X	Low	1
2	*A*31:01*	*A*33:03*	***B*44:03:02***	***B*51:02***	*01502	*02001	High	0
3	***A*24:02***	–	*B*40:01*	*B*54:01*	*01502	X	High	0
4	***A*24:02***	*A*26:02*	*B*07:02*	*B*40:06*	*00701	X	Low	1
5	*A*02:13*	*A*26:03:01*	*B*40:02*	***B*44:02***	*001	X	High	1
6	*A*11:01*	***A*24:02***	*B*40:02*	***B*51:01***	*01502	*01502	High	0
7	*A*11:01*	***A*24:02***	*B*40:01*	*B*55:02*	*00701	X	Low	1

HLA alleles with a Bw4 motif are indicated in bold.
[a]The last column shows the KIR3DS1 gene copy number.
–, donor homozygous for the HLA allele; X, donor had only one copy of the KIR3DL1 gene.

~3 wk incubation in the presence of 0.5 μM of imatinib, an imatinib-resistant subline was obtained. Introduction of the T315I mutation was confirmed by direct sequence of the PCR products between intron 5 and 6 of *ABL1* gene.

Establishment of single HLA-expressing K562 cell lines

HLA class I alleles *A*24:02*, *B*35:01*, *B*40:04*, *B*44:03*, *B*51:01*, and *B*52:01* were transduced separately into HLA-null K562 (K562-null) and K562-null with T315I mutation cells using a ViraPower Lentiviral Expression System (Thermo Fisher Scientific; cat. no. K5330-00). After selection with 5 μg/ml blasticidin (FUJIFILM Wako Pure Chemical; cat. no. 029-18701) for 2 wk, single HLA-transduced K562 cells were stained with anti-HLA class I PE (clone W6/32, BioLegend, San Diego, CA; cat. no. 311406), and the highly HLA-expressing cells were sorted using a FACSAria (BD Biosciences, San Jose, CA). B*35:01 and B*40:02 have a Bw6 motif, B*44:03 a Bw4-80T motif, and A*24:01, B*51:01, and B*52:01 a Bw4-80I motif.

Generation of KIR3DL1-expressing NK-92

To make a KIR3DL1-expressing NK cell line, a lentiviral expression vector and lentiviral particles bearing *KIR3DL1*01502* cDNA (National Center for Biotechnology Information reference sequence: NM_001322168.1) were prepared by VectorBuilder Japan (Yokohama, Japan). The expression vector drives bicistronic *KIR3DL1*01502* and *GFP* transcription, which are linked by IRES sequence under the control of EF1A promoter (vector identifier [ID]: VB200713-2329wjm). The GFP control lentiviral particles (vector ID: VB160109-10005) were used as a mock. NK-92 was infected with lentiviral particles along with 4 μg/ml of polybrene (Nacalai Tesque; cat. no. 12996-81) and 6 μM of PDK-1 inhibitor BX-795 (Selleck Chemicals, Houston, TX; cat. no. S1274) (38). Virus-infected cells were sorted as GFP-positive cells with a FACSAriaII (BD Biosciences) for use in subsequent experiments.

PBMCs from healthy donors and patients

Peripheral blood from healthy volunteers and CML patients was obtained with written informed consent in accordance with the guidelines of the World Medical Association's Declaration of Helsinki. PBMCs were isolated using Lympholyte-H (Cedarlane Laboratories, Burlington, Ontario, Canada; cat. no. CL5026) following the manufacturer's protocol. NK cells were isolated using an NK Cell Isolation Kit, human (Miltenyi Biotec, Bergisch Gladbach, Germany; cat. no. 130-092-657) following the manufacturer's protocol. This study was approved by the institutional review board of Kyoto University Hospital (accession ID: G0697-16, https://kyoto.bvits.com/rinri/publish_document.aspx?ID=1898).

HLA/KIR genotyping

HLA-A and *-B* alleles were determined using a WAKFlow HLA Typing kit (Wakunaga Pharmaceuticals, Hiroshima, Japan; cat. no. 4N705 and 4N805), which is based on PCR sequence–specific oligonucleotide probes coupled with multiple analyte profiling technology (Luminex 100 System, Luminex, Austin, TX). The primer sequences in the kit are specifically designed for each HLA locus. The *HLA* alleles were assigned automatically using the WAKFlow typing software (Wakunaga Pharmaceuticals). *KIR3DL1* genotyping was performed by GenoDive Pharma (Atsugi, Japan). Briefly, the *KIR* gene region (18 *KIR* genes including *KIR3DL1*) was enriched by the capture method (captured by hybridization using an artificially synthesized DNA probe) and then sequenced by Miseq (Illumina, San Diego, CA).

Flow cytometry

Cells were suspended in Dulbecco PBS (Nacalai Tesque; cat. no. 14249-24) supplemented with 1% FBS and incubated with

PBMCs from a KIR3DL1-high donor were coincubated with K562-null and HLA-transduced K562 cell lines at the indicated effector to target (E:T) ratios (10:1, 3:1, and 1:1). The percentages of the $CD107a^+$ $KIR3DL1^+$ and $KIR3DL1^-$ NK cells were plotted. Representative data from three independent experiments are shown. CD107a expression, as a marker of degranulation activity, was measured in triplicate samples in each experiment. Error bars show the SEM. (**D**) Representative contour plots showing CD107a expression levels of $KIR3DL1^+$ NK cells from four donors (KIR3DL1-low, no. 1 and no. 4; KIR3DL1-high, no. 2 and no. 3) challenged by K562-null, B*44:03, or B*52:01 transduced K562 cells at an E:T ratio of 1:1. (**E**) The percentage of $CD107a^+$ $KIR3DL1^+$ NK cells from all seven donors are presented as the mean value of triplicate samples. Error bars show the SEM. *$p < 0.05$, **$p < 0.01$, ***$p < 0.001$. FSC, forward scatter; ns, not significant.

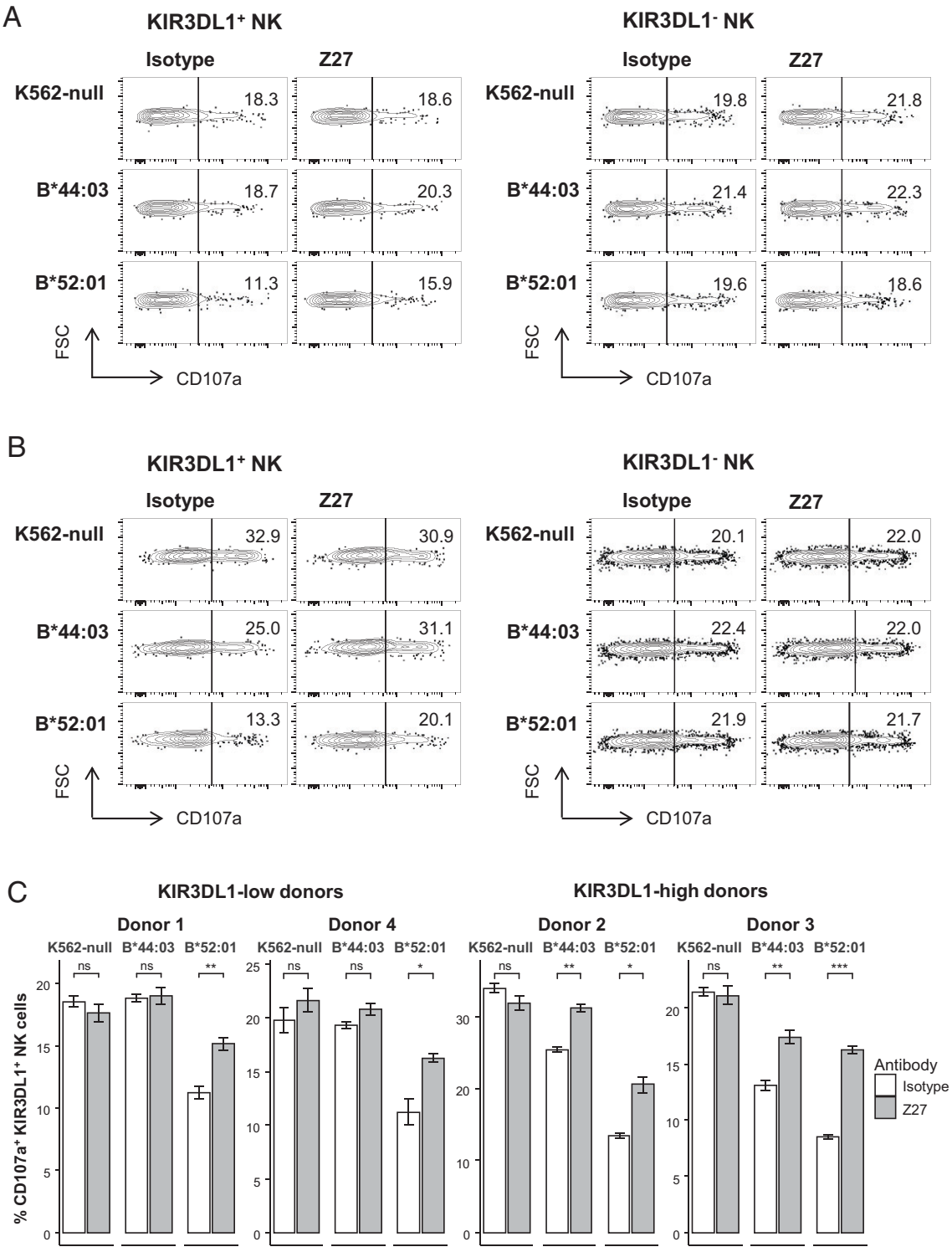

FIGURE 2. Anti-KIR3DL1 Ab reverses inhibition of KIR3DL1+ NK cells by HLA-B.

The levels of CD107a expression as a marker of degranulation activity of KIR3DL1$^+$ and KIR3DL1$^-$ NK cells challenged by K562-null, B*44:03, or B*52:01 transduced K562 cells in the presence of Z27 or isotype control Abs were measured. Representative flow cytometry contour plots of a KIR3DL1-low donor (no. 1) (**A**) and a KIR3DL1-high donor (no. 2) (**B**) are presented. (**C**) The percentages of CD107a$^+$KIR3DL1$^+$ NK cells from four donors are presented as the mean value of triplicate samples. Error bars show the SEM. *$p < 0.05$, **$p < 0.01$, ***$p < 0.001$. FSC, forward scatter; ns, not significant.

https://doi.org/10.4049/immunohorizons.2100054

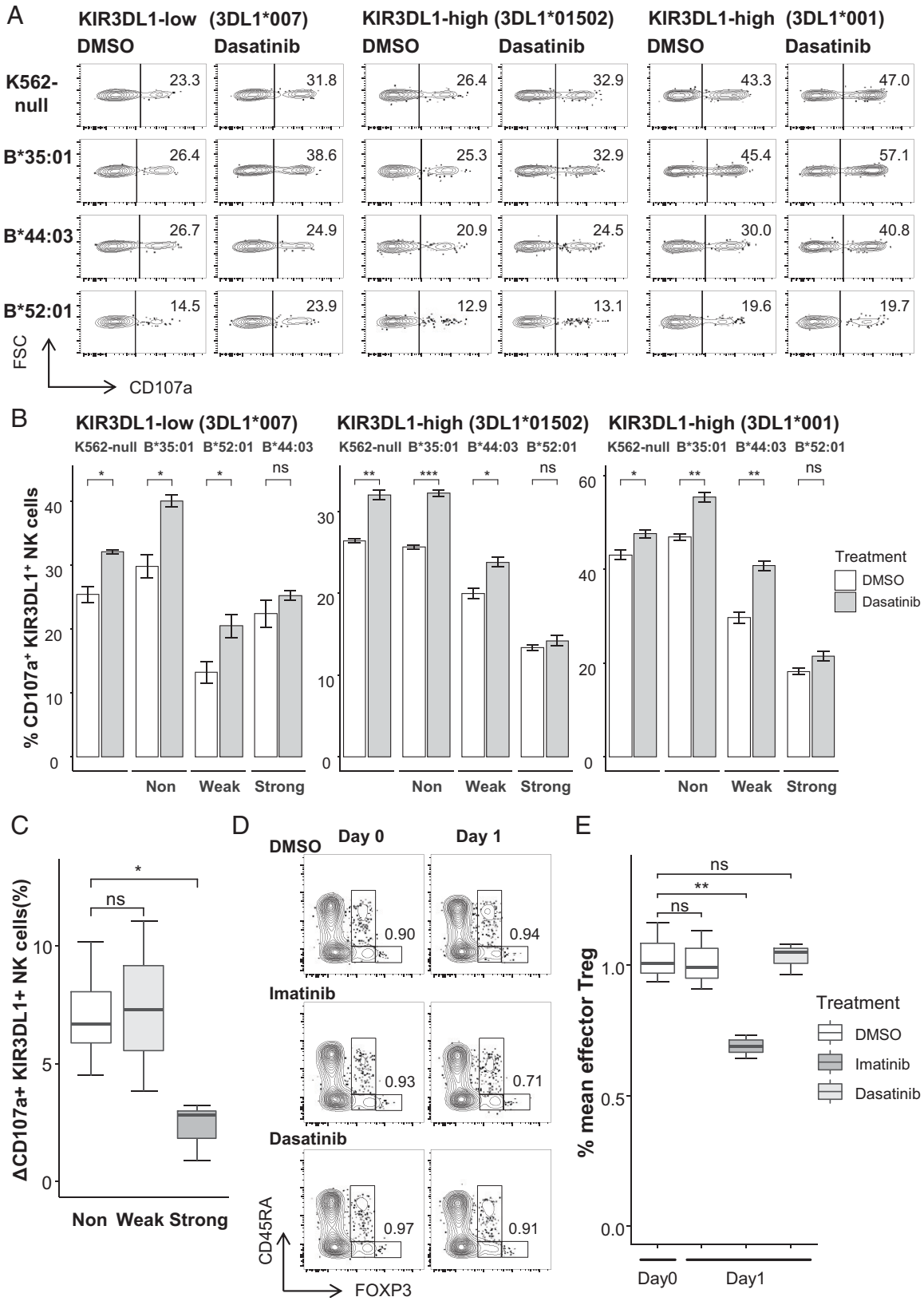

FIGURE 3. Dasatinib differentially activates NK cells depending on the combination of KIR3DL1 and HLA-B allotypes.

PBMCs from healthy donors were treated with 1 nM dasatinib or DMSO and then cocultured with K562-null or HLA-B–transduced K562 cells at an effector:target ratio of 1:1. (**A**) Representative flow cytometry contour plots showing the levels of CD107a as a marker of degranulation ***(Continued)***

Abs. For intracellular staining of FOXP3, cells were fixed and permeabilized using a Foxp3/Transcription Factor Staining Buffer Set (eBioscience; cat. no. 00-5523-00). For intracellular staining of phosphorylated ERK1/2, cells were fixed with FIX & PERM Fixation Medium A (Invitrogen; cat. no. GAS001S100) and permeabilized with FIX & PERM Fixation Medium B (Invitrogen; cat. no. GAS002S100). The following Abs were used: anti-CD3 allophycocyanin/H7 (clone SK7, BD Biosciences; cat. no. 641397), anti-CD16 FITC (clone NKP15, BD Biosciences; cat. no. 347523), anti-CD56 PerCP/Cy5.5 (clone B159, BD Biosciences; cat. no. 560842), anti-CD158e1 allophycocyanin (clone DX9, BD Biosciences; cat. no. 564103), anti-CD107a PE and allophycocyanin (clone H4A3, BioLegend; cat. no. 328608 and no. 328620, respectively), anti-CD158e1e2 PE (clone Z27, Beckman Coulter, Brea, CA; cat. no. IM3292), anti-HLA ABC PE (clone DX17, BD Biosciences; cat. no. 560168), anti-CD45RA FITC (clone HI100, BioLegend; cat. no. 304106), anti-CD4 PerCP/Cy5.5 (clone SK3, BD Biosciences; cat. no. 341654), anti-CD25 PE/Cy7 (clone M-A251, BD Biosciences; cat. no. 560920), anti-FOXP3 allophycocyanin (clone 236A/E7, eBioscience, Thermo Fisher Scientific; cat. no. 17-4777-42), anti–phospho-p44/42 MAPK (Erk1/2; clone D13.14.4E, Cell Signaling Technology, Danvers, MA; cat. no. 4370), and donkey anti-rabbit IgG (H+L) IgG Alexa Fluor 647 (Invitrogen; cat. no. A31573). Data were acquired using a FACSLyric (BD Biosciences) or FACSCanto II (BD Biosciences) flow cytometer and analyzed with FlowJo software (BD Biosciences).

Measurement of NK cell activity

The activation status of NK cells was evaluated by staining CD107a, which is expressed by lytic granules. PBMCs from healthy donors or patients were cocultured with K562-null or single HLA-expressing K562 cells to induce NK cell activation. Anti-CD107a Ab was added, followed by 5 h incubation, during which monensin (BioLegend; cat. no. 420701) was added after 1 h. $CD3^-CD56^+$ lymphocytes were gated as NK cells, and the percentage of $CD107a^+$ cells among $KIR3DL1^+$ and $KIR3DL1^-$ NK cells was measured. For blocking experiments, 0.1 μg/ml of Z27 (anti-KIR3DL1/S1) Ab was added to effector cells prior to coincubation, depending on previous reports with modification (31,39). Purified mouse IgG1 (clone MOPC-21, BD Biosciences; cat. no. 555746) was used as an isotype control. To prevent nonspecific binding of Abs, PBMCs or NK cells were pretreated with human BD Fc Block (BD Biosciences; cat. no. 564220), following the manufacturer's protocol. For experiments using dasatinib, effector cells were treated with appropriate concentrations of dasatinib (Selleck Chemicals; cat. no. S1021) or DMSO (Nacalai Tesque; cat. no. 13408-64) for 24 h. Coculture with target cell lines was started after washing out the drugs.

Measurement of effector Tregs

$FOXP3^{high}CD45RA^-$ populations among CD4 T cells were defined as effector Tregs. PBMCs from healthy donors were treated with 5 μM imatinib (Selleck Chemicals; cat. no. S2475), 1 nM dasatinib, or DMSO for 24 h. The percentages of effector Tregs before and after treatment were measured by flow cytometry.

Killing assay

Target cells were labeled with CellTrace CFSE (Invitrogen; cat. no. C34554) or CellTrace Violet (CTV; Invitrogen; cat. no. C34557) at a final concentration of 2 μM. After incubation with effector cells for 48 h, dead target cells were stained using LIVE/DEAD Fixable Near-IR Dead Cell Stain Kit (Invitrogen; cat. no. L34975). Target cell killing was evaluated by calculating the dead cell percentage (those expressing LIVE/DEAD) among CFSE- or CTV-positive cells.

Statistical analysis

Student *t* test was used to compare mean values of two independent groups. Three or more groups were compared with one-way ANOVA test. A p value < 0.05 was considered statistically significant. All statistical analysis was performed using R software (version 3.6.3, R Foundation for Statistical Computing, Vienna, Austria).

RESULTS

Activation of $KIR3DL1^+$ NK cells depends on KIR3DL1 expression

We first determined the expression levels of KIR3DL1 protein on NK cells in seven healthy donors using two different clones of anti-KIR3DL1 Abs, DX9 and Z27. The donors could be

activity in $KIR3DL1^+$ NK cells. The KIR3DL1 allele of each donor (donors no. 4, no. 3, and no. 5) is indicated in parentheses. (**B**) The percentages of $CD107a^+$ $KIR3DL1^+$ NK cells are presented as the mean value of triplicate samples. The interaction strength between KIR3DL1 and HLA-B is indicated in the bottom of the graph. Error bars show the SEM. $*p < 0.05$, $**p < 0.01$, $***p < 0.001$. (**C**) The increase in the percentage of $CD107a^+$ $KIR3DL1^+$ NK cells from three healthy donors after treatment with dasatinib is presented as a box–whisker plot. The interaction strength of the KIR3DL1 and HLA-B interactions are indicated below the graph. Boxes represent the interquartile range, the horizontal lines in the boxes indicate the median value, and the whiskers indicate the minimum and maximum values. $*p < 0.05$. (**D** and **E**) Analysis of Tregs after treatment with TKIs, imatinib, and dasatinib. PBMCs from healthy donors were treated with DMSO, 5 μM imatinib, or 1 nM dasatinib. The percentage of $FOXP3^{high}$ $CD45RA^-$ cells (effector Treg population) among $CD4^+$ lymphocytes was measured on days 0 and 1. (D) Representative contour plots of $CD4^+$ lymphocytes from a single donor. (E) The mean percentages of effector Tregs from three healthy donors under each treatment condition are presented as box–whisker plots. Boxes represents interquartile range, horizontal lines in the boxes represent the median value, and whiskers indicate the minimum and the maximum values. $**p < 0.01$. FSC, forward scatter; ns, not significant.

https://doi.org/10.4049/immunohorizons.2100054

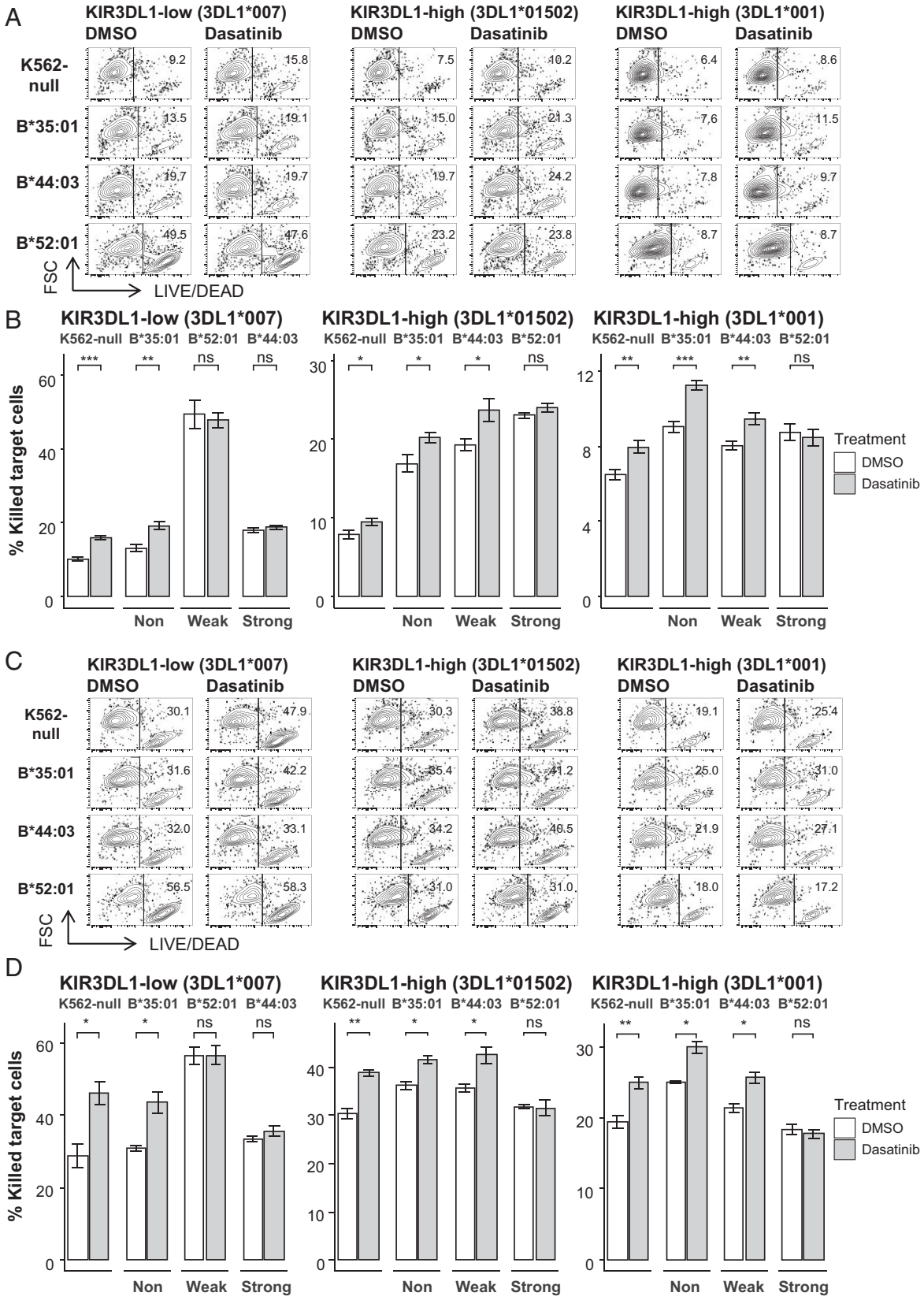

FIGURE 4. Dasatinib enhances NK cell cytotoxicity in the context of KIR3DL1 and HLA-B noninteracting pairs.

(**A** and **B**) PBMCs from healthy donors were treated with 1 nM dasatinib or DMSO and then cocultured with K562-null or HLA-B–transduced K562 cells at an effector:target ratio of 4:1. (A) Representative flow cytometry contour plots showing the dead cells after gating on ***(Continued)***

divided into two groups according to the mean fluorescence intensity (MFI) of Z27 staining (Fig. 1A). Donors no. 1, no. 4, and no. 7 showed low MFI of Z27, and donors no. 2, no. 3, no. 5, and no. 6 showed high MFI of Z27 (Fig. 1B). *KIR3DL1* and *HLA-A* and *-B* alleles of these donors were determined (Table I). All donors with *KIR3DL1*00701* showed low MFI of Z27 (KIR3DL1-low donors), and donors with other alleles including **01502* showed high MFI of Z27 (KIR3DL1-high donors).

We next examined activation of NK cells from these donors. PBMCs from a KIR3DL1-high donor were challenged with K562-null and specific HLA-transduced K562 cells (hereafter, these cell lines are described by the HLA-B alleles they express). CD107a expression as a surrogate marker of degranulation activity of KIR3DL1$^+$ and KIR3DL1$^-$ NK cells was measured by flow cytometry. Degranulation activity levels increased as the ratio of effector:target decreased (Fig. 1C). Activation of KIR3DL1$^+$ NK cells was more affected by HLA-B alleles on target K562 cells than was activation of KIR3DL1$^-$ NK cells.

Activation of KIR3DL1$^+$ NK cells from the seven donors was measured. CD107a expression after coculture with K562-null was used as a reference, and activation of KIR3DL1$^+$ NK cells against two HLA-B–transduced K562 cells was different depending on the KIR3DL1 expression levels. NK cells from KIR3DL1-low donors showed no inhibition by B*44:03, which has the Bw4-80T allotype, but were inhibited by B*52:01, which has the Bw4-80I allotype. NK cells from KIR3DL1-high donors showed inhibition both by B*44:03 and B*52:01 (Fig. 1D, 1E).

Anti-KIR3DL1 Ab reverses inhibition of KIR3DL1$^+$ NK cells by HLA-B

To verify that NK cell inhibition depends on physical ligation of KIR3DL1 by HLA-B, PBMCs were first treated with anti-KIR3DL1/S1 Ab Z27 or an isotype control and then cocultured with the target K562 cells. Degranulation (as represented by CD107a expression) of KIR3DL1$^+$ NK cells from KIR3DL1-low donors was inhibited by B*52:01, which was reversed by Z27 Ab (Fig. 2A). Similarly, Z27 Ab blocked the inhibition of KIR3DL1$^+$ NK cells from KIR3DL1-high donors by B*44:03 and B*52:01 (Fig. 2B). The blocking effect was similar within the two groups (Fig. 2C). Z27 Ab had little effect on degranulation activity of KIR3DL1$^-$ NK cells from either group.

Dasatinib differentially activates NK cells depending on the combination of KIR3DL1 and HLA-B allotypes

We next examined the effect of dasatinib on NK cell activity. Dasatinib enhanced NK cell activity against K562-null cells at specific concentrations (Supplemental Fig. 1A, 1B). PBMCs from healthy donors were treated with 1 nM dasatinib and then cocultured with K562-null or HLA-transduced K562 cells. Dasatinib enhanced degranulation of KIR3DL1$^+$ NK cells against K562-null cells and those transduced with B*35:01, which had the Bw6 allotype, in each of three donors (donors no. 4, no. 3, and no. 5; the same applies hereafter) with different KIR3DL1 alleles (Fig. 3A, upper two rows). After dasatinib treatment, KIR3DL1$^+$ NK cells from a *KIR3DL1*007* donor showed increased degranulation activity against B*52:01 (Bw4-80I) but not against B*44:03 (Bw4-80T) cells. By contrast, KIR3DL1$^+$ NK cells from *KIR3DL1*01502* and **001* donors showed increased degranulation activity against B*44:03 (Bw4-80T) but not against B*52:01 (Bw4-80I) cells (Fig. 3A, lower two rows). According to the classification of binding strength between KIR3DL1 and HLA-B, which was defined in previous clinical studies (30,31,34), the combinations in which dasatinib enhanced degranulation were weak or noninteracting pairs (Fig. 3B, 3C; the classification of KIR3DL1 and HLA-B pairs in this experiment is summarized in Supplemental Table 1).

Because the PBMCs included T cells as effectors, we examined the effects of dasatinib on Tregs. Whereas treatment with 5 μM imatinib for 1 d decreased the percentage of effector Tregs, treatment with 1 nM dasatinib did not change the effector Treg frequencies (Fig. 3D, 3E). These results indicate that dasatinib-induced NK cell activation is not associated with Treg numbers.

Dasatinib enhances NK cell cytotoxicity in the context of KIR3DL1 and HLA-B noninteracting pairs

To examine whether increased expression of CD107a as a surrogate marker of degranulation is associated with enhanced cytotoxicity, target cell lysis was evaluated by flow cytometry. PBMCs from donors with *KIR3DL1*007*, **01502*, or **001* alleles were treated with dasatinib and then cocultured with a series of K562 cells as target cells. Dasatinib enhanced cell lysis by PBMCs from a KIR3DL1-low donor (**007*) against K562-null and B*35:01 (Bw6) cells but did not change against B*44:03 (Bw4-80T) and B*52:01 (Bw4-80I) cells (Fig. 4A). In contrast, dasatinib enhanced cell lysis by PBMCs from KIR3DL1-high donors (**01502* and **001*) against K562-null, B*35:01 (Bw6),

CFSE-traced target cells. The KIR3DL1 allele of each donor (donors no. 4, no. 3, and no. 5) is indicated in parentheses. Cells positive for the LIVE/DEAD stain are dead cells. (B) The percentages of lysed target cells are presented as the mean value of triplicate samples. The interaction strength between KIR3DL1 and HLA-B is indicated in the bottom of the graph. Error bars show the SEM. *$p < 0.05$, **$p < 0.01$, ***$p < 0.001$. (**C**, **D**) NK cells were isolated from PBMCs of healthy donors and used as effectors. Freshly isolated NK cells were treated with 1 nM dasatinib or DMSO and then cocultured with K562-null or HLA-B–transduced K562 cells at an effector:target ratio of 1:1. (C) Representative contour plots showing the dead cells among CFSE-traced target cells. The KIR3DL1 allele of each donor is indicated in parentheses. (D) The percentages of lysed target cells are presented as the mean value of triplicate samples. The interaction strength between KIR3DL1 and HLA-B is indicated in the bottom of the graph. Error bars show the SEM. *$p < 0.05$, **$p < 0.01$, ***$p < 0.001$. FSC, forward scatter; ns, not significant.

https://doi.org/10.4049/immunohorizons.2100054

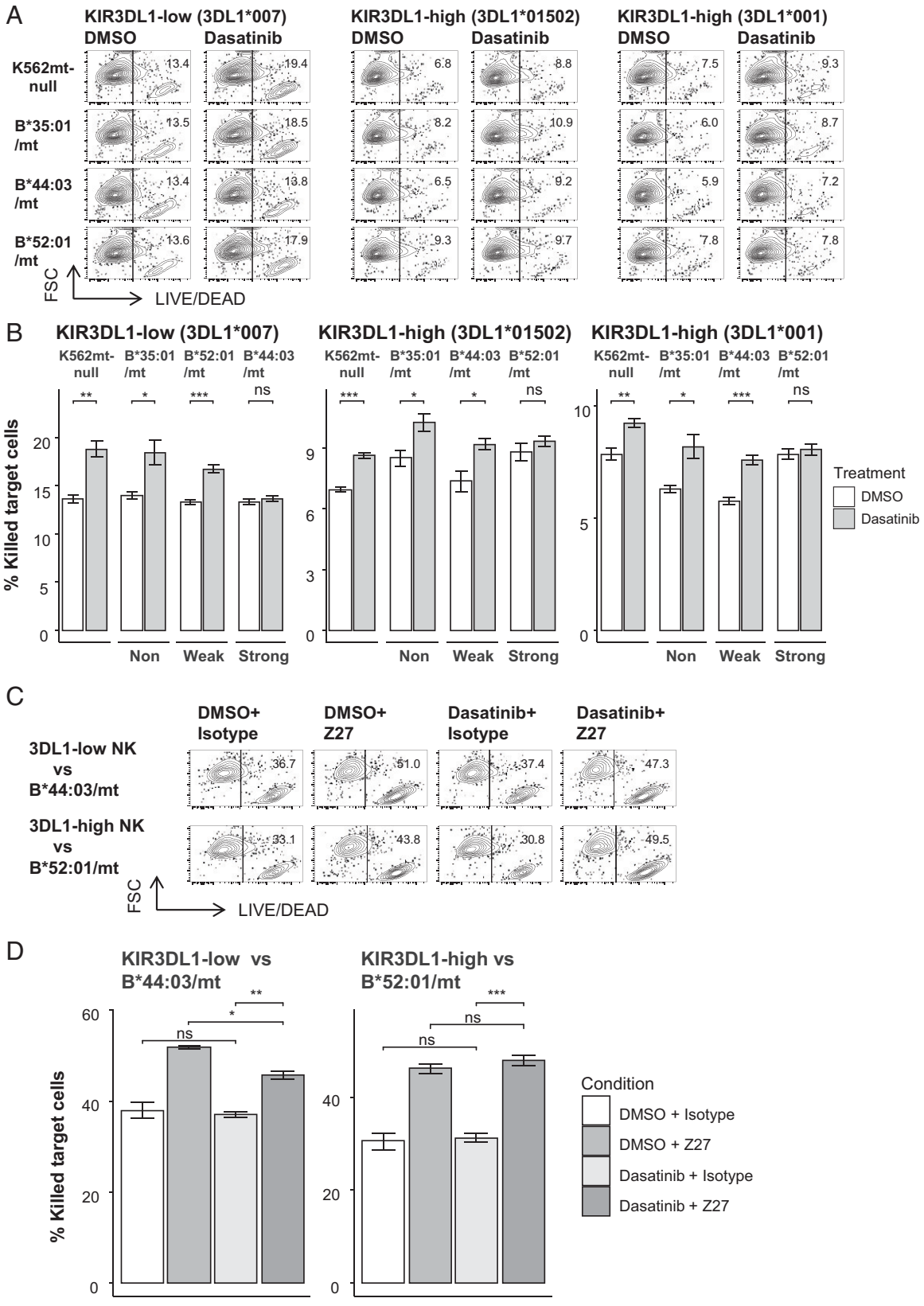

FIGURE 5. Dasatinib enhances NK cell cytotoxicity against K562 cells with the BCR-ABL1 T315I mutation.

(**A** and **B**) PBMCs from healthy donors were treated with 1 nM dasatinib or DMSO and then cocultured with mutant (mt; bearing the T315I mutation) K562-null or HLA-B–transduced K562 cells at the effector:target ratio of 4:1. (A) Representative flow cytometry contour plots showing ***(Continued)***

and B*44:03 (Bw4-80T) cells (Fig. 4A). Target cell lysis was enhanced only in the context of noninteracting pairs in the KIR3DL1-low donors and with non- and weak-interacting pairs in the KIR3DL1-high donors (Fig. 4B). To confirm that NK cells were the main contributor to the lytic effects, we isolated NK cells from healthy donors and used them as effectors. The results were similar to those obtained from coculture of whole PBMCs and K562 cells (Fig. 4C, 4D).

Dasatinib enhances NK cell cytotoxicity against K562 cells with the BCR-ABL1 T315I mutation

To verify whether dasatinib enhances lysis of CML cells with the T315I mutation, we used T315I knock-in mutants of K562-null and HLA-B–transduced K562 cells as targets. When dasatinib-treated PBMCs from a KIR3DL1-low donor (**007*) were cultured as effectors, target cell lysis was increased against mutant K562-null, mutant B*35:01 (Bw6), and mutant B*52:01 (Bw4-80I) cells but unchanged against mutant B*44:03 (Bw4-80T) cells (Fig. 5A). By contrast, when PBMCs from KIR3DL1-high donors (**01502* and **001*) were cultured as effectors, target cell lysis was increased against mutant K562-null, B*35:01 (Bw6), and B*44:03 (Bw4-80T) cells (Fig. 5A). The enhancement of target cell lysis occurred in the context of non- and weak-interacting pairs (Fig. 5B).

We next blocked interaction between KIR3DL1 and HLA-B in strong-interacting pairs using the anti-KIR3DL1 Ab Z27. NK cells from KIR3DL1-low and KIR3DL1-high donors were isolated and treated with dasatinib before coincubation with CFSE-traced target cells in the presence of Z27. Z27 addition resulted in enhanced target cell lysis by NK cells with or without dasatinib (Fig. 5C), but synergistic effects of dasatinib and Z27 were not seen against mutant K562 cells (Fig. 5D).

*NK cell line expressing KIR3DL1*01502 allotype shows an activation pattern against target cells similar to primary NK cells*

KIR3DL1$^+$ NK cells from healthy donors may express other KIR proteins, which makes it difficult to evaluate the function of KIR3DL1 protein. Therefore, functional analysis using a KIR3DL1-negative NK-92 cell line and a KIR3DL1-transduced counterpart was performed. A KIR3DL1-high allele cDNA (*KIR3DL1*01502*) was introduced into NK-92 cells with a lentiviral vector along with GFP (NK-92-3DL1; Fig. 6A), and GFP-transduced NK-92 cells (NK-92-MOCK) were prepared as a control. Coculture with K562 cells resulted in activation of NK-92 cells as evaluated by flow cytometric analysis of CD107a expression as a marker of degranulation activity. Degranulation activity of NK-92-3DL1 cells was inhibited when the target K562 cells expressed B*44:03 or B*52:01, whereas the control NK-92-MOCK cells were not inhibited by these HLA-B allotypes (Fig. 6B). The inhibition by B*52:01 was stronger than by B*44:03. We also assessed intracellular signaling by measuring phosphorylation levels of ERK1/2. Phospho-ERK1/2 levels were suppressed within NK-92-3DL1 cells when challenged with B*44:03 and B*52:01 cells but not K562-null cells (Fig. 6C). The activation pattern of NK-92-3DL1 cells was consistent with that of KIR3DL1-high primary NK cells (Fig. 6D). To confirm KIR3DL1-mediated modulation of NK-92 cells, target cell lysis was evaluated in the presence of Z27 Ab. Whereas cytotoxicity of NK-92-3DL1 cells was reduced by B*44:03 and B*52:01, the addition of Z27 Ab restored cytotoxic activity (Fig. 6E, 6F).

Activation of NK cells from CML patients depends on the expression levels of KIR3DL1

CD107a expression was measured by flow cytometry to assess degranulation activity by KIR3DL1$^+$ NK cells from four CML patients against K562 cells. In addition, we also determined expression levels of KIR3DL1 protein by Z27 MFI. Depending on these analyses, we examined whether the patterns of degranulation activity were consistent with those of the healthy donors. When a patient had both KIR3DL1-low and KIR3DL1-high populations, these were separately analyzed (Fig. 7A). Six populations of KIR3DL1$^+$ NK cells from four patients were analyzed (Fig. 7B, 7C). All KIR3DL1-low populations showed inhibition only by B*52:01, and all KIR3DL1-high populations showed the inhibition by B*44:03 and B*52:01 (Fig. 7D). These results were consistent with the results obtained from healthy donors (Fig. 1D, 1E).

DISCUSSION

In this study, we showed that NK cell activity and cytotoxicity against K562 cells was modulated by physical interaction between KIR3DL1 and HLA-B proteins in healthy donors and CML patients (Figs. 1, 2, and 7). In addition, we showed that dasatinib enhanced NK cell activity and cytotoxicity in a KIR3DL1 allotype-dependent manner (Figs. 3 and 4), which is consistent with the findings of our previous clinical study (34). This concept was also confirmed against target cells harboring the BCR-ABL1 T315I mutation (Fig. 5). Furthermore, we proved that blocking an interaction between specific KIR3DL1

the dead cells among CFSE-traced target cells. The KIR3DL1 allele of each donor (donors no. 4, no. 3, and no. 5) is indicated in parentheses. (B) The percentages of lysed target cells are presented as the mean value of triplicate samples. The interaction strength between KIR3DL1 and HLA-B is indicated in the bottom of the graph. Error bars show the SEM. *$p < 0.05$, **$p < 0.01$, ***$p < 0.001$. (**C** and **D**) NK cells were isolated from PBMCs of healthy donors and used as effectors. Freshly isolated NK cells were treated with 1 nM dasatinib or DMSO. After Fc blocking, drug-treated NK cells were cocultured with mt K562-null or HLA-B–transduced K562 cells (strong-interacting pairs) at an effector:target ratio of 1:1 in the presence of 0.1 μg/ml isotype control or Z27 Ab. (D) The percentages of lysed target cells are presented as the mean value of triplicate samples. Error bars show the SEM. *$p < 0.05$, **$p < 0.01$, ***$p < 0.001$. FSC, forward scatter; ns, not significant.

https://doi.org/10.4049/immunohorizons.2100054

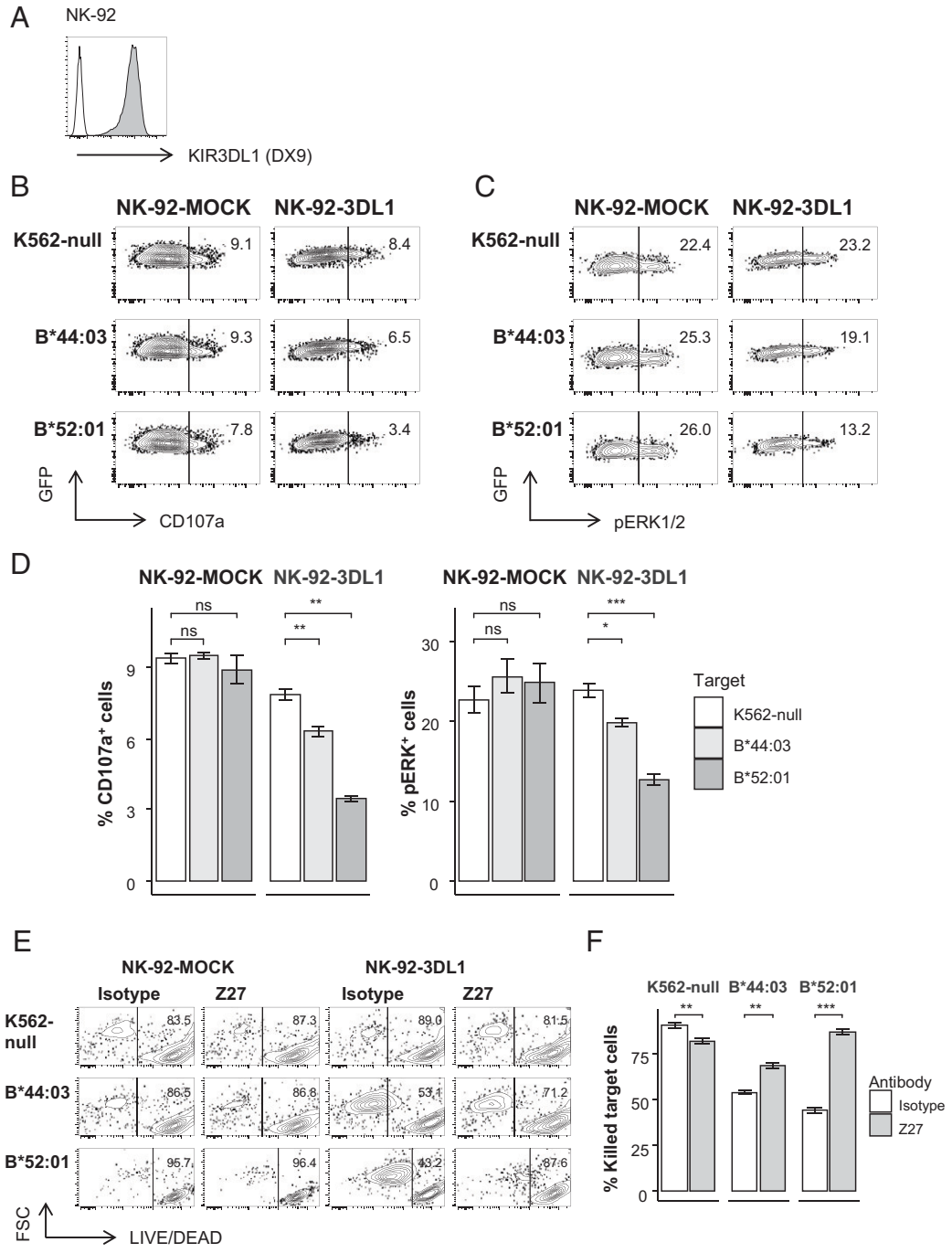

FIGURE 6. NK cell line expressing KIR3DL1*01502 allotype shows an activation pattern against target cells similar to primary NK cells.
(**A**) Histogram showing the expression levels of KIR3DL1 on mock-transduced (white) and *KIR3DL1*01502*-transduced (gray) NK-92 cells. (**B** and **C**) The activation of the NK-92 cell line after coincubation with K562-null, B*44:03, or B*52:01 transduced K562 cells was evaluated by flow cytometry measuring CD107a expression levels (B) and ERK1/2 phosphorylation levels (C). Representative contour plots are shown. (**D**) Levels of expression of CD107a as a marker of NK-92 activation are presented as the mean value of triplicated samples. Error bars show the SEM. *$p < 0.05$, **$p < 0.01$, ***$p < 0.001$. (**E** and **F**) Target cell lysis by mock-/KIR3DL1-transduced NK-92 was evaluated. Target cells were traced with CTV dye and then coincubated with NK-92 effector cells in the presence of 0.1 μg/ml isotype control or Z27 Abs. (E) Representative contour plot showing the percentage of dead cells in each condition. (F) The percentages of lysed target cells are presented as the mean value of triplicate samples. Error bars show the SEM. *$p < 0.05$, **$p < 0.01$, ***$p < 0.001$. FSC, forward scatter; NK-92-3DL1, KIR3DL1*01502-transduced NK-92; NK-92-MOCK, mock-transduced NK-92; ns, not significant.

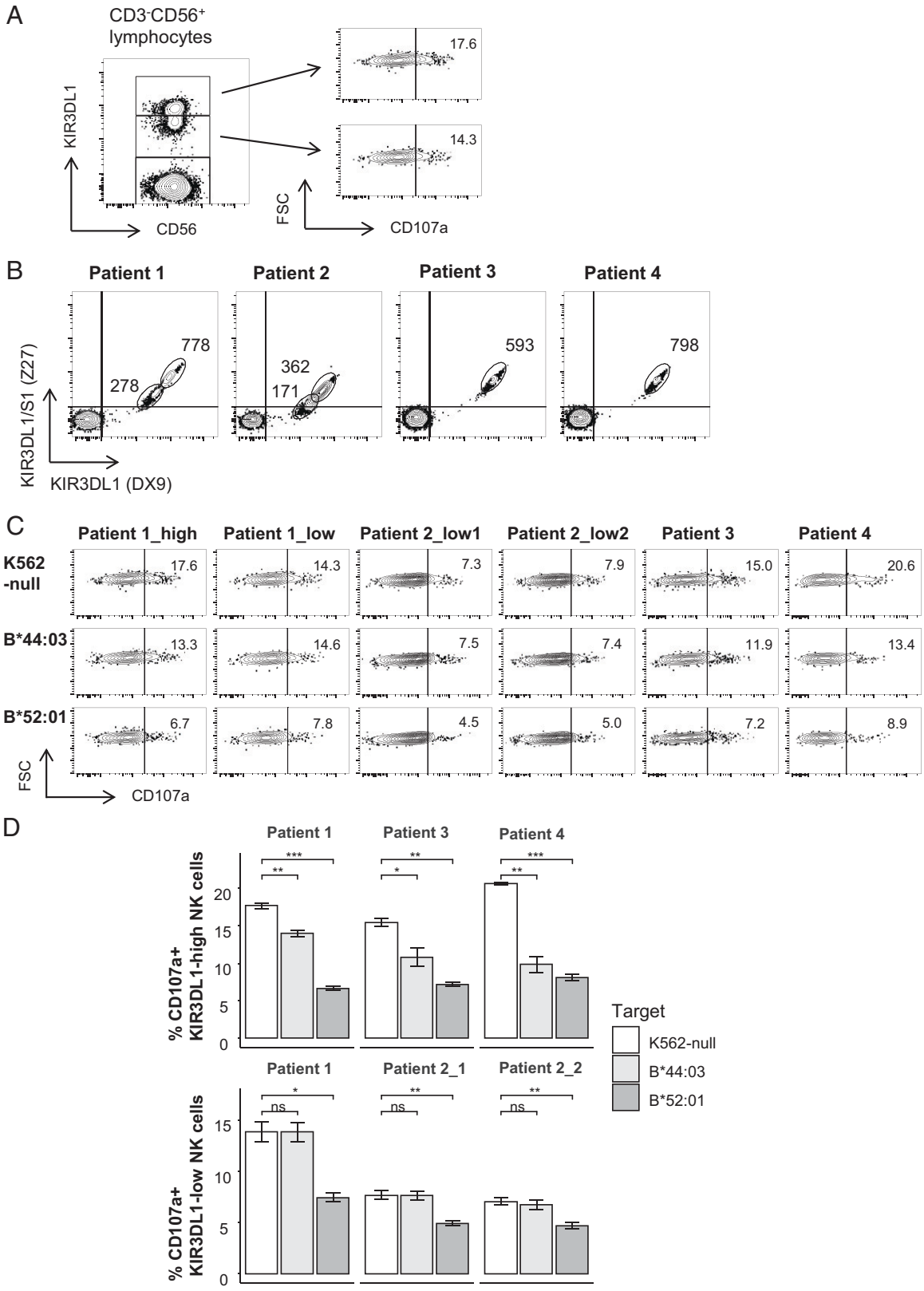

FIGURE 7. NK cells from CML patients show differential activating patterns depending on the expression levels of KIR3DL1.

(**A**) A representative flow cytometry contour plot showing the gating for KIR3DL1-high and -low NK cell populations. CD107a expression levels as a marker of degranulation activity of each population after challenge with the K562-null target cells are shown on the right as ***(Continued)***

https://doi.org/10.4049/immunohorizons.2100054

and HLA proteins could enhance target cell lysis (Fig. 6). These results provide a strong rationale for KIR3DL1 allotypes as therapeutic targets for optimizing treatment of CML and possibly for use to improve treatments of other cancers.

Activation of KIR3DL1$^+$ NK cells against K562 cells was differentially inhibited depending on HLA-B allotypes on the target cells, and this inhibition could be classified into two patterns according to the expression levels of KIR3DL1 protein on the effector cells. Furthermore, KIR3DL1 blocking by Z27 Ab reversed the inhibition. Thus, the combination of KIR3DL1 allotype and HLA-B alleles regulates activity of KIR3DL1$^+$ NK cells. Although the combination of Bw4-80T and KIR3DL1-low allotypes is classified as a strong-interacting pair, KIR3DL1-low NK cells bearing the **007* allele were not inhibited by Bw4-80T HLA-B*44:03 (Fig. 1). However, after treatment with dasatinib, the KIR3DL1*007 and B*44:03 pairing showed no enhancement of cytotoxicity in agreement with the classification (Figs. 3, 4). The classification was originally derived from a clinical study (29), and the affinity between KIR3DL1 and HLA-B allotype molecules measured by tetramer binding assay are not always true for these definitions (39). Notably, our results indicate that modulation of NK cell immunity through KIR3DL1 and HLA can be altered in the presence of dasatinib, which has as an immunomodulatory function.

Boudreau et al. (28) showed slightly stronger binding of 3DL1*007 and *015 tetramers to B*44:03 than to B*52:01. Saunders et al. (39) reported similar results from tetramer binding assays. Results published by Foley et al. (40) demonstrated stronger inhibition of both 3DL1-high (*015) and -low (*005-like) NK cells by B*44:03 than by B*52:01. However, in our experiment, B*52:01 showed stronger inhibition of both 3DL1-high (*015) and -low (*007) NK cells than B*44:03. This discrepancy may be attributable to differences in target cell lines. All previous research used EBV-transformed B-LCL (721.221) cells as the target, whereas we used K562 cells. It is now assumed that 721.221 cell line does not completely lack HLA class I expression, whereas our data confirm that K562 cells completely lack HLA class I expression. Therefore, we consider that K562 cells are more suitable for analyzing KIR–HLA interactions. Tremblay-McLean et al. (41) showed that K562 cells express several ligands for activating NKG2D receptor, whereas 721.221 cells do not, which may also affect NK cell activation.

It has been reported that imatinib and dasatinib activate NK cell immunity through suppression of Tregs (35,36). Treg suppression was not apparent at the concentration of dasatinib used in our experiments, suggesting another mechanism of NK cell activation by dasatinib. Although we have not elucidated the mechanistic details, Chang et al. (42) observed downregulation of NKG2A, another inhibitory receptor on NK cells, in CML patients who took dasatinib and showed that dasatinib downregulates NKG2A through inhibition of p38 MAPK. These results imply a direct effect of dasatinib on NK cell activation and also suggests that NK cells may be more dependent on signals from KIRs in the presence of dasatinib. In addition, enhancement of NK cell immunity by dasatinib was also shown against K562 cells with the BCR-ABL1 T315I mutation, which is naturally resistant to dasatinib. Even when the KIR–HLA combination was a strong-interacting pair, inhibition of KIR–HLA binding resulted in enhanced killing. These results suggest a possible strategy to overcome TKI resistance in CML by targeting and modulating the KIR3DL1–HLA interaction.

This study has several limitations. First, our previous research suggested that the *KIR3DL1*005* allele has a significant positive impact on the therapeutic effects of TKIs (34). However, as none of our volunteer donors carried the *KIR3DL1*005* allele, we could not verify its function and specificity in vitro. We assumed that the NK cell activation pattern would be similar for those of the *005 and *007 allotypes because they share the KIR3DL1-low phenotype, although this remains to be verified. Second, as NK cell effects are an aggregate of multiple KIR–HLA interactions, our in vitro results cannot be translated directly into clinical practice, and validation in a large clinical study is needed. Third, we could not examine how dasatinib affected KIR3DL1–HLA interactions and modulated NK cell activity in detail. Despite these limitations, our results are sufficient to indicate the importance of NK cell modulation through KIR–HLA interactions during CML therapy.

Therapeutic blockade of the inhibitory KIRs on NK cells is an attractive way to enhance antitumor NK cell immunity. Its feasibility has been explored using the Ab lirilumab, which targets KIR2DL1/2/3. However, although promising results were reported in a mouse model (43), a recent phase Ib clinical trial for relapsed or refractory lymphoid malignancies failed to show additional benefits of lirilumab on PD-1 blockade (44). Intervention at the level of KIR3DL1–HLA binding could be an alternative option for a novel immune checkpoint therapy. Several studies mention that blocking inhibitory KIRs including

examples. (**B**) Representative contour plots of KIR3DL1$^+$ NK cells stained with Z27 and DX9 Abs. The difference in MFI (δ MFI) between positive and negative populations was calculated for each population and indicated as a number in the plots. (**C**) PBMCs from four CML patients were coincubated with K562-null, B*44:03, or B*52:01 transduced K562 cells at an effector:target ratio of 1:1. Representative contour plots showing the expression levels of CD107a in KIR3DL1$^+$ NK cells. The KIR3DL1$^+$ populations that had δ MFI more than 500 were classified as KIR3DL1-high populations, and the populations that had δ MFI fewer than 500 were classified as KIR3DL1-low populations. Patient 1 had a KIR3DL1-high (Patient 1_high) and KIR3DL1-low (Patient 1_low) populations. Patient 2 had two KIR3DL1-low populations, which are indicated as Patient 2_low1 (the δ MFI is 171) and Patient 2_low2 (the δ MFI is 362). (**D**) The percentages of CD107a$^+$ cells among high and low KIR3DL1$^+$ NK cells are presented as the mean value of triplicate samples. Patient 2_1 and Patient 2_2 refer to the Patient 2_low 1 population and Patient 2_low2 population, respectively. Error bars show the SEM. $*p < 0.05$, $**p < 0.01$, $***p < 0.001$; ns, not significant.

KIR3DL1 could enhance NK cell cytotoxicity (15, 30,39,45). Our study not only confirmed these results but also showed the significance of KIR3DL1 blocking in the presence of a TKI. Furthermore, we showed that KIR3DL1 blocking was effective even in TKI-resistant cells, providing a new treatment strategy for patients with CML that has acquired drug-resistant mutations. Notably, our results also suggest that appropriate patient selection based on the KIR3DL1 alleles could maximize the efficacy of KIR3DL1 blockade. Only a limited number of KIR–HLA pairs were examined in our study, and a more detailed analysis of KIR–HLA interactions, including validation in a large clinical study, should be conducted to optimize NK cell immunity against CML and other malignancies.

DISCLOSURES

T.S. received research grants from Novartis Pharmaceuticals Foundation and Bristol-Myers Squibb Foundation. A.T-K. received research funds and lecture fees from Novartis Pharmaceuticals Foundation, Takeda Pharmaceutical Co., Ltd., Otsuka Pharmaceutical Co., Ltd., Pfizer Inc., and Bristol-Myers Squibb. The other authors have no financial conflicts of interest.

ACKNOWLEDGMENTS

The authors deeply thank Kimiko Yurugi (Kyoto University Hospital) for HLA typing and Mari Morita (Kyoto University Graduate School of Medicine) for excellent discussions.

REFERENCES

1. Hochhaus, A., R. A. Larson, F. Guilhot, J. P. Radich, S. Branford, T. P. Hughes, M. Baccarani, M. W. Deininger, F. Cervantes, S. Fujihara, et al. IRIS Investigators. 2017. Long-term outcomes of imatinib treatment for chronic myeloid leukemia. *N. Engl. J. Med.* 376: 917–927.
2. Bower, H., M. Björkholm, P. W. Dickman, M. Höglund, P. C. Lambert, and T. M. L. Andersson. 2016. Life expectancy of patients with chronic myeloid leukemia approaches the life expectancy of the general population. *J. Clin. Oncol.* 34: 2851–2857.
3. Patel, A. B., T. O'Hare, and M. W. Deininger. 2017. Mechanisms of resistance to ABL kinase inhibition in chronic myeloid leukemia and the development of next generation ABL kinase inhibitors. *Hematol. Oncol. Clin. North Am.* 31: 589–612.
4. Efficace, F., and L. Cannella. 2016. The value of quality of life assessment in chronic myeloid leukemia patients receiving tyrosine kinase inhibitors. *Hematology (Am. Soc. Hematol. Educ. Program).* 2016: 170–179.
5. Padula, W. V., R. A. Larson, S. B. Dusetzina, J. F. Apperley, R. Hehlmann, M. Baccarani, E. Eigendorff, J. Guilhot, F. Guilhot, R. Hehlmann, et al. 2016. Cost-effectiveness of tyrosine kinase inhibitor treatment strategies for chronic myeloid leukemia in chronic phase after generic entry of imatinib in the United States. *J. Natl. Cancer Inst.* 108: djw003.
6. Yamamoto, C., H. Nakashima, T. Ikeda, S.-I. Kawaguchi, Y. Toda, S. Ito, K. Mashima, T. Nagayama, K. Umino, D. Minakata, et al. 2019. Analysis of the cost-effectiveness of treatment strategies for CML with incorporation of treatment discontinuation. *Blood Adv.* 3: 3266–3277.
7. Etienne, G., J. Guilhot, D. Rea, F. Rigal-Huguet, F. Nicolini, A. Charbonnier, A. Guerci-Bresler, L. Legros, B. Varet, M. Gardembas, et al. 2017. Long-term follow-up of the French Stop Imatinib (STIM1) study in patients with chronic myeloid leukemia. *J. Clin. Oncol.* 35: 298–305.
8. Imagawa, J., H. Tanaka, M. Okada, H. Nakamae, M. Hino, K. Murai, Y. Ishida, T. Kumagai, S. Sato, K. Ohashi, et al. DADI Trial Group. 2015. Discontinuation of dasatinib in patients with chronic myeloid leukaemia who have maintained deep molecular response for longer than 1 year (DADI trial): a multicentre phase 2 trial. *Lancet Haematol.* 2: e528–e535.
9. Ilander, M., U. Olsson-Strömberg, H. Schlums, J. Guilhot, O. Brück, H. Lähteenmäki, T. Kasanen, P. Koskenvesa, S. Söderlund, M. Höglund, et al. 2016. Increased proportion of mature NK cells is associated with successful imatinib discontinuation in chronic myeloid leukemia. *Leukemia.* 31: 1108–1116.
10. Anfossi, N., P. André, S. Guia, C. S. Falk, S. Roetynck, C. A. Stewart, V. Breso, C. Frassati, D. Reviron, D. Middleton, et al. 2006. Human NK cell education by inhibitory receptors for MHC class I. *Immunity.* 25: 331–342.
11. Ljunggren, H.-G., and K. Kärre. 1990. In search of the 'missing self': MHC molecules and NK cell recognition. *Immunol. Today.* 11: 237–244.
12. Horowitz, A., Z. Djaoud, N. Nemat-Gorgani, J. Blokhuis, H. G. Hilton, V. Béziat, K. J. Malmberg, P. J. Norman, L. A. Guethlein, and P. Parham. 2016. Class I HLA haplotypes form two schools that educate NK cells in different ways. *Sci. Immunol.* 1: eaag1672.
13. Garcia, C. A., J. Robinson, L. A. Guethlein, P. Parham, J. A. Madrigal, and S. G. E. Marsh. 2003. Human KIR sequences 2003. *Immunogenetics.* 55: 227–239.
14. Middleton, D., and F. Gonzelez. 2010. The extensive polymorphism of KIR genes. *Immunology.* 129: 8–19.
15. Litwin, V., J. Gumperz, P. Parham, J. H. Phillips, and L. L. Lanier. 1994. NKB1: a natural killer cell receptor involved in the recognition of polymorphic HLA-B molecules. *J. Exp. Med.* 180: 537–543.
16. Wan, A. M., P. Ennis, P. Parham, and N. Holmes. 1986. The primary structure of HLA-A32 suggests a region involved in formation of the Bw4/Bw6 epitopes. *J. Immunol.* 137: 3671–3674.
17. Müller, C. A., G. Engler-Blum, V. Gekeler, I. Steiert, E. Weiss, and H. Schmidt. 1989. Genetic and serological heterogeneity of the supertypic HLA-B locus specificities Bw4 and Bw6. *Immunogenetics.* 30: 200–207.
18. Gumperz, J. E., V. Litwin, J. H. Phillips, L. L. Lanier, and P. Parham. 1995. The Bw4 public epitope of HLA-B molecules confers reactivity with natural killer cell clones that express NKB1, a putative HLA receptor. *J. Exp. Med.* 181: 1133–1144.
19. Gardiner, C. M., L. A. Guethlein, H. G. Shilling, M. Pando, W. H. Carr, R. Rajalingam, C. Vilches, and P. Parham. 2001. Different NK cell surface phenotypes defined by the DX9 antibody are due to KIR3DL1 gene polymorphism. *J. Immunol.* 166: 2992–3001.
20. Pando, M. J., C. M. Gardiner, M. Gleimer, K. L. McQueen, and P. Parham. 2003. The protein made from a common allele of KIR3DL1 (3DL1*004) is poorly expressed at cell surfaces due to substitution at positions 86 in Ig domain 0 and 182 in Ig domain 1. *J. Immunol.* 171: 6640–6649.
21. Trundley, A., H. Frebel, D. Jones, C. Chang, and J. Trowsdale. 2007. Allelic expression patterns of KIR3DS1 and 3DL1 using the Z27 and DX9 antibodies. *Eur. J. Immunol.* 37: 780–787.
22. Thomas, R., E. Yamada, G. Alter, M. P. Martin, A. A. Bashirova, P. J. Norman, M. Altfeld, P. Parham, S. K. Anderson, D. W. McVicar, and M. Carrington. 2008. Novel KIR3DL1 alleles and their expression levels on NK cells: convergent evolution of KIR3DL1 phenotype variation? *J. Immunol.* 180: 6743–6750.

23. Sharma, D., K. Bastard, L. A. Guethlein, P. J. Norman, N. Yawata, M. Yawata, M. Pando, H. Thananchai, T. Dong, S. Rowland-Jones, et al. 2009. Dimorphic motifs in D0 and D1+D2 domains of killer cell Ig-like receptor 3DL1 combine to form receptors with high, moderate, and no avidity for the complex of a peptide derived from HIV and HLA-A*2402. *J. Immunol.* 183: 4569–4582.
24. Parham, P., P. J. Norman, L. Abi-Rached, and L. A. Guethlein. 2011. Variable NK cell receptors exemplified by human KIR3DL1/S1. *J. Immunol.* 187: 11–19.
25. Carr, W. H., M. J. Pando, and P. Parham. 2005. KIR3DL1 polymorphisms that affect NK cell inhibition by HLA-Bw4 ligand. *J. Immunol.* 175: 5222–5229.
26. Yawata, M., N. Yawata, M. Draghi, A. M. Little, F. Partheniou, and P. Parham. 2006. Roles for HLA and KIR polymorphisms in natural killer cell repertoire selection and modulation of effector function. *J. Exp. Med.* 203: 633–645.
27. O'Connor, G. M., K. J. Guinan, R. T. Cunningham, D. Middleton, P. Parham, and C. M. Gardiner. 2007. Functional polymorphism of the KIR3DL1/S1 receptor on human NK cells. *J. Immunol.* 178: 235–241.
28. Boudreau, J. E., T. J. Mulrooney, J.-B. Le Luduec, E. Barker, and K. C. Hsu. 2016. KIR3DL1 and HLA-B Density and Binding Calibrate NK Education and Response to HIV. *J. Immunol.* 196: 3398–3410.
29. Martin, M. P., Y. Qi, X. Gao, E. Yamada, J. N. Martin, F. Pereyra, S. Colombo, E. E. Brown, W. L. Shupert, J. Phair, et al. 2007. Innate partnership of HLA-B and KIR3DL1 subtypes against HIV-1. *Nat. Genet.* 39: 733–740.
30. Forlenza, C. J., J. E. Boudreau, J. Zheng, J. B. Le Luduec, E. Chamberlain, G. Heller, N. K. V. Cheung, and K. C. Hsu. 2016. KIR3DL1 allelic polymorphism and HLA-B epitopes modulate response to Anti-GD2 monoclonal antibody in patients with neuroblastoma. *J. Clin. Oncol.* 34: 2443–2451.
31. Boudreau, J. E., F. Giglio, T. A. Gooley, P. A. Stevenson, J. B. Le Luduec, B. C. Shaffer, R. Rajalingam, L. Hou, C. K. Hurley, H. Noreen, et al. 2017. KIR3DL1/HLA-B subtypes govern acute myelogenous leukemia relapse after hematopoietic cell transplantation. *J. Clin. Oncol.* 35: 2268–2278.
32. Schetelig, J., H. Baldauf, F. Heidenreich, C. Massalski, S. Frank, J. Sauter, M. Stelljes, F. A. Ayuk, W. A. Bethge, G. Bug, et al. 2020. External validation of models for KIR2DS1/KIR3DL1-informed selection of hematopoietic cell donors fails. *Blood.* 135: 1386–1395.
33. Boudreau, J. E., and K. C. Hsu. 2018. Natural killer cell education in human health and disease. *Curr. Opin. Immunol.* 50: 102–111.
34. Ureshino, H., T. Shindo, H. Kojima, Y. Kusunoki, Y. Miyazaki, H. Tanaka, H. Saji, A. Kawaguchi, and S. Kimura. 2018. Allelic polymorphisms of KIRs and HLAs predict favorable responses to tyrosine kinase inhibitors in CML. *Cancer Immunol. Res.* 6: 745–754.
35. Tanaka, A., H. Nishikawa, S. Noguchi, D. Sugiyama, H. Morikawa, Y. Takeuchi, D. Ha, N. Shigeta, T. Kitawaki, Y. Maeda, et al. 2020. Tyrosine kinase inhibitor imatinib augments tumor immunity by depleting effector regulatory T cells. *J. Exp. Med.* 217: e20191009.
36. Hekim, C., M. Ilander, J. Yan, E. Michaud, R. Smykla, M. Vähä-Koskela, P. Savola, S. Tähtinen, L. Saikko, A. Hemminki, et al. 2017. Dasatinib changes immune cell profiles concomitant with reduced tumor growth in several murine solid tumor models. *Cancer Immunol. Res.* 5: 157–169.
37. Tamai, M., T. Inukai, S. Kojika, M. Abe, K. Kagami, D. Harama, T. Shinohara, A. Watanabe, H. Oshiro, K. Akahane, et al. 2018. T315I mutation of BCR-ABL1 into human Philadelphia chromosome-positive leukemia cell lines by homologous recombination using the CRISPR/Cas9 system. *Sci. Rep.* 8: 9966.
38. Sutlu, T., S. Nyström, M. Gilljam, B. Stellan, S. E. Applequist, and E. Alici. 2012. Inhibition of intracellular antiviral defense mechanisms augments lentiviral transduction of human natural killer cells: implications for gene therapy. *Hum. Gene Ther.* 23: 1090–1100.
39. Saunders, P. M., P. Pymm, G. Pietra, V. A. Hughes, C. Hitchen, G. M. O'Connor, F. Loiacono, J. Widjaja, D. A. Price, M. Falco, et al. 2016. Killer cell immunoglobulin-like receptor 3DL1 polymorphism defines distinct hierarchies of HLA class I recognition. *J. Exp. Med.* 213: 791–807.
40. Foley, B. A., D. De Santis, E. Van Beelen, L. J. Lathbury, F. T. Christiansen, and C. S. Witt. 2008. The reactivity of Bw4+ HLA-B and HLA-A alleles with KIR3DL1: implications for patient and donor suitability for haploidentical stem cell transplantations. *Blood.* 112: 435–443.
41. Tremblay-McLean, A., S. Coenraads, Z. Kiani, F. P. Dupuy, and N. F. Bernard. 2019. Expression of ligands for activating natural killer cell receptors on cell lines commonly used to assess natural killer cell function. *BMC Immunol.* 20: 8.
42. Chang, M. C., H. I. Cheng, K. Hsu, Y. N. Hsu, C. W. Kao, Y. F. Chang, K. H. Lim, and C. G. Chen. 2019. NKG2A down-regulation by dasatinib enhances natural killer cytotoxicity and accelerates effective treatment responses in patients with chronic myeloid leukemia. *Front. Immunol.* 9: 3152.
43. Kohrt, H. E., A. Thielens, A. Marabelle, I. Sagiv-Barfi, C. Sola, F. Chanuc, N. Fuseri, C. Bonnafous, D. Czerwinski, A. Rajapaksa, et al. 2014. Anti-KIR antibody enhancement of anti-lymphoma activity of natural killer cells as monotherapy and in combination with anti-CD20 antibodies. *Blood.* 123: 678–686.
44. Armand, P., A. Lesokhin, I. Borrello, J. Timmerman, M. Gutierrez, L. Zhu, M. Popa McKiver, and S. M. Ansell. 2020. A phase 1b study of dual PD-1 and CTLA-4 or KIR blockade in patients with relapsed/refractory lymphoid malignancies. *Leukemia.* 35: 777–786.
45. Binyamin, L., R. K. Alpaugh, T. L. Hughes, C. T. Lutz, K. S. Campbell, and L. M. Weiner. 2008. Blocking NK cell inhibitory self-recognition promotes antibody-dependent cellular cytotoxicity in a model of anti-lymphoma therapy. *J. Immunol.* 180: 6392–6401.

Supplementary table 1: Definitions for interaction between KIR3DL1 and HLA-B allotypes in this experiment

		KIR3DL1		
		*00701	*01502	*001
HLA-B	B*35:01	non	non	non
	B*44:03	strong	weak	weak
	B*52:01	weak	strong	strong

The above classification is defined by adopting the definition in previous clinical studies (see references 30, 31, and 34 in the main text). In brief, any pair that contains Bw6 is classified as non, 3DL1-low to Bw4-80I pairs and 3DL1-high to Bw4-80T pairs are classified as weak, and 3DL1-low to Bw4-80T pairs and 3DL1-high to Bw4-80I pairs are classified as strong.

Figure S1

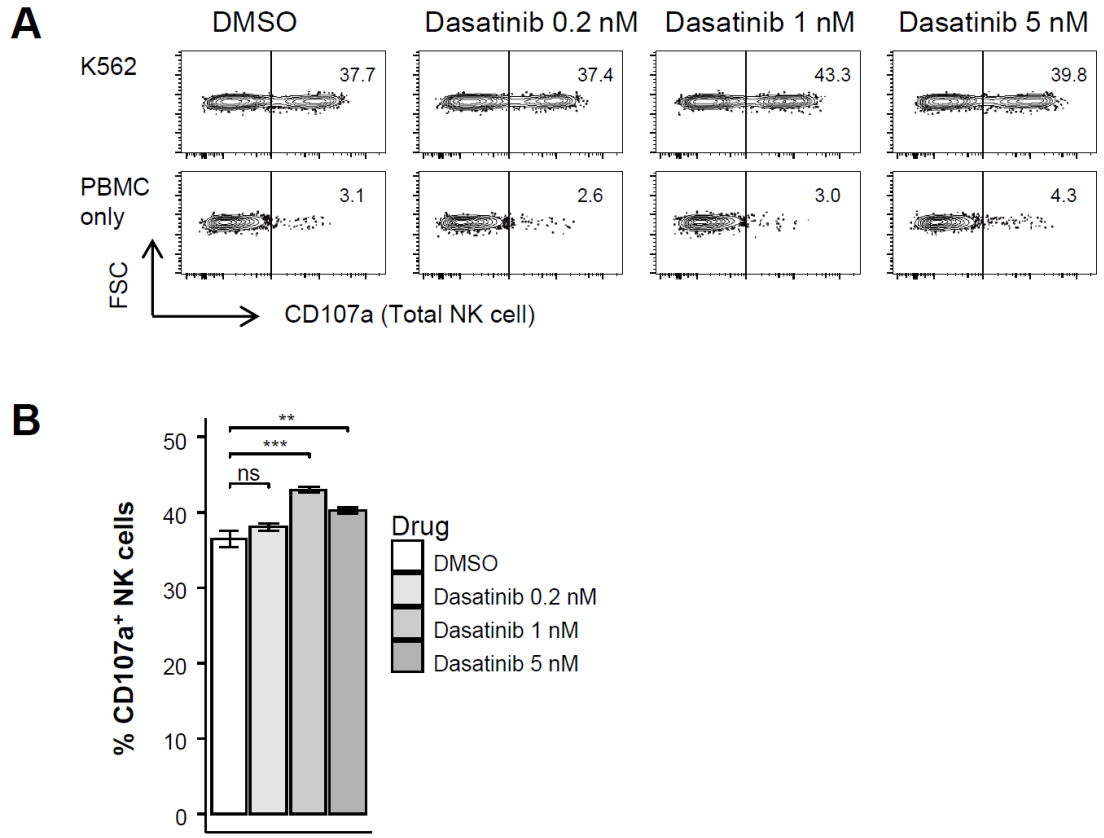

Supplementary figure 1: Pretreatment of NK cells with dasatinib increases CD107a expression levels

(A) Representative flow cytometry contour plots showing the expression level of CD107a (as a marker of degranulation activity) in total NK cells. PBMCs were treated with DMSO or dasatinib for 24 hours at the indicated concentrations. After washing out of drugs, pre-treated PBMCs with or without co-incubation with K562 cells at an effector: target (E:T) ratio of 1: 1 were stained with anti-CD107a antibody. FSC, forward scatter. (B) The percentages of CD107a+ NK cells are presented as the mean value of triplicate samples. Error bars show the standard error of the mean (SEM; ns, not significant; *, P<0.05; **, P<0.01; ***, P<0.001).